

## Alkali ion migration control from flat glass substrates<sup>1)</sup>

Nikolas Janke<sup>2)</sup>, Oliver Grassmé and Rudolf Weißmann

Institut für Werkstoffwissenschaften III, Lehrstuhl Glas und Keramik, Universität Erlangen-Nürnberg, Erlangen (Germany)

---

Sodium diffusion from flat glass substrates during annealing changes properties of refined flat glass. In the case of the development of the CuInSe<sub>2</sub> thin film solar cell, annealing at 550 °C is necessary for the formation of suitable crystalline phases. Sodium diffusing from the soda–lime–silica glass substrate influences crystal growth and the main electrical parameters of the solar cell. Different possibilities in sodium ion migration control are presented, considering the influence of glass composition on sodium diffusion and its chemical potential as well as passivation of sodium-containing glasses by diffusion barriers. Experimental results in connection with the thin film solar cell show that sodium-free substrates or glass compositions which immobilise sodium at tetrahedral sites of boron oxide or alumina can be used without further surface treatment. Soda–lime–silica glass with sputter-deposited Al<sub>2</sub>O<sub>3</sub> and BiO<sub>x</sub> thin films or CVD coatings (SiN<sub>x</sub>:H, SiO<sub>x</sub>) as diffusion barrier coatings shows promise as a cheap substrate material. Alternatively, dealkalisation of soda–lime–silica glass in HCl atmosphere leads to silica-rich surfaces with excellent barrier properties. The investigations are carried out using various surface analytical tools like Auger Electron Spectroscopy (AES), X-Ray Diffractometry under Grazing Incidence (GI-XRD), high-resolution Scanning Electron Microscopy (SEM), and Fourier Transform Infrared spectroscopy (FTIR).

### Kontrolle der Diffusion von Alkaliionen aus Flachglassubstraten

Die Diffusion von Alkaliionen aus Flachglas-Substraten während einer Temperung verändert die Eigenschaften veredelter Gläser. Bei der Herstellung von CuInSe<sub>2</sub>-Dünnschichtsolarzellen ist eine Temperung bei 550 °C erforderlich, um bestimmte kristalline Phasen zu erzeugen. Natrium, das hierbei aus dem Kalk-Natronsilicatglas ausdiffundiert, beeinflusst das Kristallwachstum und die wichtigsten elektrischen Kenngrößen der Solarzelle. In der vorliegenden Arbeit werden verschiedene Möglichkeiten zur Kontrolle der Diffusion der Natriumionen aufgezeigt. Im Vordergrund steht hierbei der Einfluß der Glaszusammensetzung auf die Natriumdifffusion, d.h. auf das chemische Potential der Natriumionen, sowie die Passivierung natriumhaltiger Gläser durch Diffusionssperrschichten. Im Zusammenhang mit den experimentellen Untersuchungen an der Dünnschichtsolarzelle zeigt sich, daß natriumfreie Substrate oder Gläser, die Natrium an Bor- oder Aluminiumoxid-Tetraedern binden, ohne weitere Oberflächenbehandlung des Substrats verwendet werden können. Kalk-Natronsilicatglas, das mit über Sputterverfahren abgeschiedenen Al<sub>2</sub>O<sub>3</sub>- und BiO<sub>x</sub>-Beschichtungen bzw. CVD-Schichten (SiN<sub>x</sub>:H, SiO<sub>x</sub>) als Diffusionssperren passiviert ist, erscheint als kostengünstiges Substrat vielversprechend. Alternativ zur Passivierung durch Beschichtungen zeigen mit HCl-Gas entalkalisierte, SiO<sub>2</sub>-reiche Glasoberflächen hervorragende Barriereigenschaften. Die Untersuchungen stützen sich auf den Einsatz vielfältiger oberflächensensitiver Meßmethoden, wie Auger-Elektronen-Spektroskopie (AES), Röntgendiffraktometrie unter streifendem Einfall (GI-XRD), hochauflösende Raster-Elektronenmikroskopie (SEM) und Fourier-Transformations-Infrarot-Spektroskopie (FTIR).

---

## 1. Introduction

Properties of refined flat glass depend on the chemistry of the substrate in case of processes that include temperature steps, like calcination in sol-gel technology, deposition on heated substrates or tempering in production of safety glass. Thermally activated sodium diffusion from the glass substrate into functional coatings determines product quality and leads in many cases to degradation.

One of the first hints in literature which considers the influence of the glass composition on the properties of the deposited films was found in connection with sol-

gel deposition of TiO<sub>2</sub> thin films [1]. The composition of the substrate determines the development of different crystalline phases. Anatas was detected on alkali-free and low-sodium glass, whereas brookite was found only on soda–lime–silica glass. The different crystallisation behaviour on both alkali-containing glasses was assumed to be caused by different types of sodium bonding in the silica network.

The connection between electrical conductivity of transparent oxidic coatings and glass composition is a more prominent example for the influence of the glass composition on characteristics of a coating [2 to 4]. Sodium diffusing from the substrate raises the resistance of Transparent Conductive Oxide (TCO) coatings. In this connection, in [3] are examined SnO<sub>2</sub> thin films deposited on various glasses with sodium content up to  $c(\text{Na}_2\text{O}) = 13\%$ . After annealing, SnO<sub>2</sub> is dissolved and the sodium concentration  $c(\text{Na})$  determined by wet

---

Received 9 March 1999, revised manuscript 3 February 2000.

<sup>1)</sup> Presented in German at the 71<sup>st</sup> Annual Meeting of the German Society of Glass Technology (DGG) in Bayreuth (Germany) on 28 May 1997.

<sup>2)</sup> Now with: Vegla GmbH, Aachen.

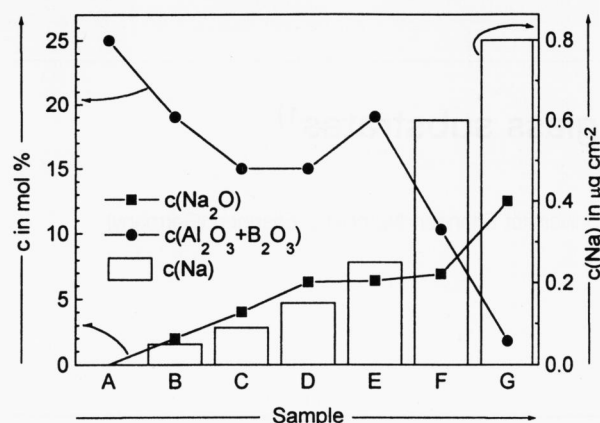


Figure 1. Non-linear relationship between sodium concentration  $c(\text{Na}_2\text{O})$  of different glass substrates A to G and sodium content  $c(\text{Na})$  of  $\text{SnO}_2$  thin films after annealing. The content of  $\text{Al}_2\text{O}_3$  and  $\text{B}_2\text{O}_3$  in the glasses is indicated as  $c(\text{Al}_2\text{O}_3 + \text{B}_2\text{O}_3)$  [3].

chemical analysis. As it is illustrated in figure 1 the amount of sodium in  $\text{SnO}_2$  increases non-linearly with the sodium content of the substrate. A relationship between sodium outlet of the substrate and concentration of boron oxide and alumina, which is discussed later on, is recognizable.

Alkali ion migration is a complex phenomenon, influenced by glass composition and thin film properties. The first part of this paper summarises fundamentals on sodium diffusion in glasses and thin films. From this, different possibilities in alkali ion migration control are derived. Furthermore, the interdiffusion mechanism is discussed, considering the chemical potential as the driving force.

In the second part, experimental results in alkali ion migration control are presented in connection with the development of a  $\text{CuInSe}_2$  (CIS) thin film solar cell. The photovoltaic multilayer is deposited on soda–lime–silica glass. Processing requires a temperature step slightly above the strain point of the substrate. Sodium diffusing into the semiconductor influences grain growth and main electrical parameters, above all the conversion efficiency. The effect of suppressing alkali ion migration from the substrate by using different glass compositions or passivated soda–lime–silica glass is investigated. Passivation is carried out by diffusion barrier coatings and dealcalisation as a chemical surface pre-treatment. Results are discussed considering the influence of glass composition on sodium outlet and thin film properties.

## 2. Interactions between glass substrates and functional coatings

Contamination of functional coatings on flat glass by ions diffusing from the substrate, above all sodium, is a complex process which is determined by the chemical composition of the substrate, the microstructure of the

Table 1. Sodium diffusion in silica glass [8]

glass type	$D_0$ in $\text{cm}^2 \text{s}^{-1}$	$Q$ in $\text{kJ mol}^{-1}$	$D_{550^\circ\text{C}}$ in $\text{cm}^2 \text{s}^{-1}$	$x_{550^\circ\text{C}}$ in $\mu\text{m}$	$c_{\text{OH}}$ in ppm
I	0.374	108.0	$5.3 \cdot 10^{-8}$	80	<4
II	1.32	112.6	$9.5 \cdot 10^{-8}$	107	$\approx 130$
III	$5.94 \cdot 10^{-3}$	147.4	$2.7 \cdot 10^{-12}$	0.6	$\approx 1300$

coating, impurities and dopants and the atmosphere during annealing. In principle, there are the following topics to consider in alkali ion migration control:

- Concentration and mobility of sodium in the glass, which determines particle flux towards the interface between glass and coating. Sodium diffusion in glasses depends on the composition, so it is necessary to get close information of the influence of different oxides on ionic mobility.
- Bonding of sodium in glasses, which influences the chemical potential as the driving force in diffusion.
- Clarifying the diffusion mechanism means to have a tool to suppress sodium outlet of a substrate.
- Sodium concentration in a coating after annealing depends on thin film material and its structure. Defects like cracks and grain boundaries force sodium diffusion.

This section summarises the compositional influence on sodium ion diffusion and types of sodium bonding in glasses. Commercially available substrates are discussed considering their composition and main physical properties. The diffusion mechanism as well as the influence of thin film properties are dealt with.

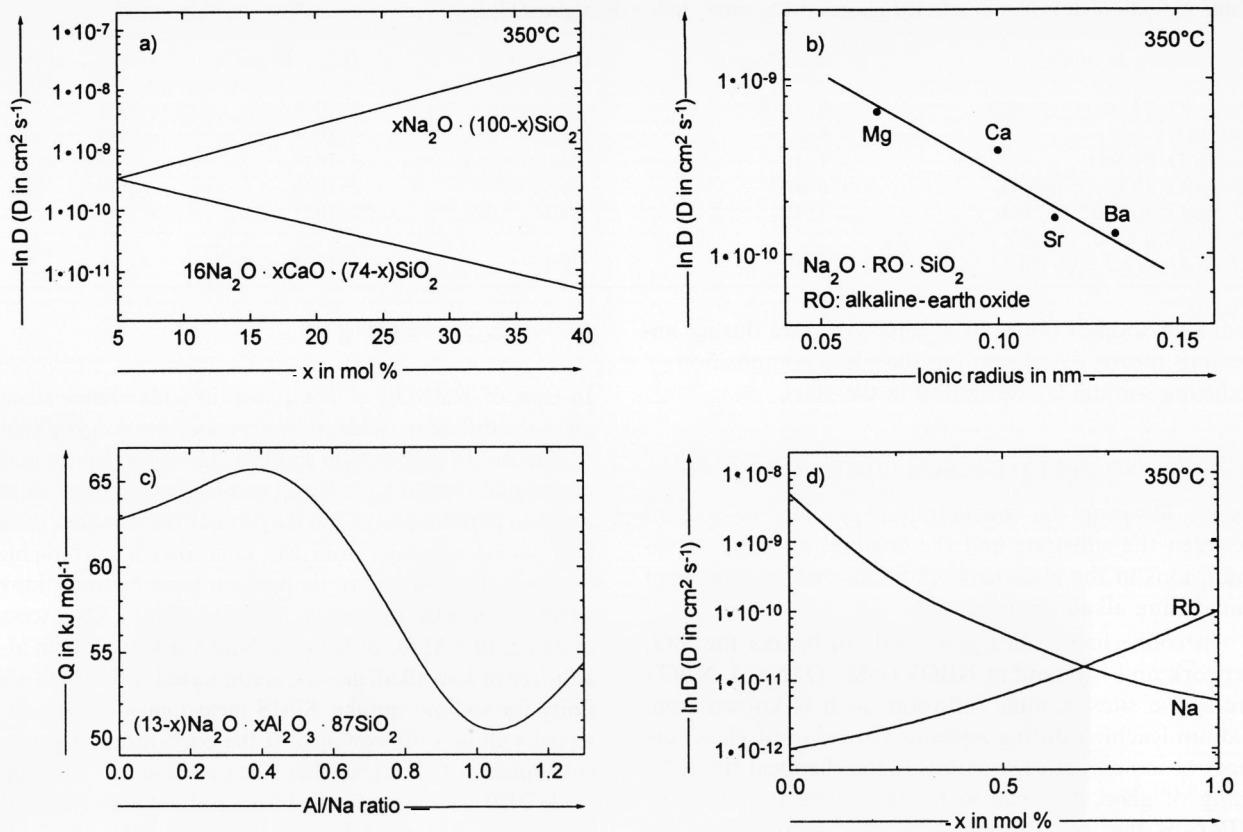
Sodium diffusion data of different materials, taken from literature, are calculated on the basis of 10 min and  $550^\circ\text{C}$ , which represents the parameters in rapid thermal processing (RTP) of the CIS thin film solar cell.

### 2.1 Mobility of alkali ions in the substrate

In the following, connections between mobility of alkali ions and glass compositions are summarised from [5 to 7]. Beginning with silica glass as the most simple glass composition, the influence of different oxides on sodium diffusion is pointed out in five steps:

#### a) Sodium diffusion in silica glass

Sodium impurity diffusion in silica glass was closely examined in the 70's [5, 8 and 9]. Table 1 summarises diffusion data for different types of silica glass, commonly indicated as I to III [8]. The diffusion coefficient at  $550^\circ\text{C}$ , which is calculated by the Arrhenius equation using the pre-exponential factor  $D_0$  and the activation energy  $Q$ , varies in three orders of magnitude. The diffusion length  $x_{550^\circ\text{C}} = \sqrt{D_{550^\circ\text{C}} t}$  gives an idea how far sodium ions can diffuse during annealing at  $550^\circ\text{C}$  for 10 min.



Figures 2a to d. Influence of glass composition on sodium diffusion in soda–lime–silica glasses for a) different sodium and lime concentrations, b) different sizes of alkaline earth ions, c) different aluminium sodium ratios, d) the mixed alkali effect [5].

Sodium diffusion in silica glass strongly depends on the concentration of hydroxyl groups  $c_{\text{OH}}$ , which are incorporated into the network during the melting process. A higher concentration of OH groups is equivalent to a decreasing diffusion coefficient, which is discussed as a pseudo mixed alkali effect between sodium and protons [9].

#### b) Concentration dependence

In binary glasses  $\text{Na}_2\text{O}-\text{SiO}_2$  the sodium diffusion coefficient increases with a higher concentration of  $\text{Na}_2\text{O}$  (figure 2a). The concentration dependence is caused by the formation of non-bridging oxygens (NBO), which act as pinpoints for ionic diffusion.

#### c) Influence of alkaline earth oxides

In ternary glass systems containing  $\text{SiO}_2$ ,  $\text{Na}_2\text{O}$  and alkaline earth oxides the sodium diffusion coefficient decreases up to two orders of magnitude with rising  $\text{CaO}$  content (figure 2a). Ions with greater ionic radii, like  $\text{Ba}^{2+}$  and  $\text{Sr}^{2+}$ , are more effective in blocking sodium than smaller ones (figure 2b).

#### d) Influence of $\text{R}_2\text{O}_3$ -type oxides

The activation energy of sodium is strongly dependent on the  $\text{Al}/\text{Na}$  ratio in ternary glasses of the composition  $\text{Na}_2\text{O}-\text{Al}_2\text{O}_3-\text{SiO}_2$  (figure 2c). In the region  $\text{Al}/\text{Na} \approx 0.4$  the activation energy is high

whereas a distinct minimum is found at  $\text{Al}/\text{Na} = 1$ , which is commonly discussed as a change in coordination of aluminium.

#### e) Mixed alkali effect

The exchange of  $\text{Na}_2\text{O}$  for other alkali oxides decreases the diffusion coefficient due to steric hindrance, which is known as the mixed alkali effect (figure 2d).

Considering the connections between glass composition and ionic diffusion, we can derive the following principles for the development of glass compositions with low sodium outlet:

- = low sodium concentration,
- = addition of alkaline earth oxides, above all  $\text{SrO}$  and  $\text{BaO}$ ,
- = addition of  $\text{Al}_2\text{O}_3$  and  $\text{B}_2\text{O}_3$ ,
- = exchange of  $\text{Na}_2\text{O}$  for  $\text{K}_2\text{O}$ .

Diffusion data elucidate the effect of compositional changes for glasses with low sodium outlet. The diffusion coefficient of sodium in different glass compositions between pure silica and soda–lime–silica glass is in the range of  $D_{550^\circ\text{C}} \approx (10^{-8} \text{ to } 10^{-9}) \text{ cm}^2 \text{ s}^{-1}$ , which is equivalent to a diffusion direction  $x_{550^\circ\text{C}}$  up to  $100 \mu\text{m}$  (table 2). In any case, sodium mobility in glasses is high enough to ensure diffusion towards the interface in processing of the CIS thin film solar cell. As a consequence,

Table 2. Sodium diffusion in selected glasses (SLS: soda–lime–silica glass) [7]

composition in mol%	$D_0$ in $\text{cm}^2 \text{s}^{-1}$	$Q$ in $\text{kJ mol}^{-1}$	$D_{550^\circ\text{C}}$ in $\text{cm}^2 \text{s}^{-1}$	$x_{550^\circ\text{C}}$ in $\mu\text{m}$
29 $\text{Na}_2\text{O}$ , 14 $\text{Al}_2\text{O}_3$ , 57 $\text{SiO}_2$	$8 \cdot 10^{-4}$	62.4	$9 \cdot 10^{-8}$	103
100 $\text{SiO}_2$	0.4	108.0	$5 \cdot 10^{-8}$	80
13 $\text{Na}_2\text{O}$ , 87 $\text{SiO}_2$	$1 \cdot 10^{-3}$	72.0	$3 \cdot 10^{-8}$	62
20 $\text{Na}_2\text{O}$ , 10 $\text{CaO}$ , 70 $\text{SiO}_2$	$6 \cdot 10^{-3}$	86.3	$2 \cdot 10^{-8}$	48
20 $\text{Na}_2\text{O}$ , 10 $\text{BaO}$ , 70 $\text{SiO}_2$	$3 \cdot 10^{-2}$	99.7	$2 \cdot 10^{-8}$	41
13 $\text{Na}_2\text{O}$ , 8 $\text{CaO}$ , 4 $\text{MgO}$ , 0.6 $\text{Al}_2\text{O}_3$ , 72.2 $\text{SiO}_2$ (SLS)	$1 \cdot 10^{-2}$	98.4	$6 \cdot 10^{-9}$	26

reducing sodium outlet of a glass substrate during annealing means – concerning the glass composition – reducing sodium concentration in the glass.

## 2.2 Sodium sites in glasses: chemical potential

Beside lowering the concentration gradient of sodium between the substrate and the coating, trapping of sodium ions in the glass network is another possibility of minimising alkali ion migration.

In soda–lime–silica glass, sodium breaks the  $\text{SiO}_4$  network and is bound at NBO's ( $\equiv\text{Si}-\text{O}^-\text{Na}^+$ ). NBO's are active sites in ionic diffusion, as it is known from sodium leaching during aqueous corrosion of glass surfaces or ion exchange reactions in the chemical strengthening of glass. The reason for the active behaviour of NBO's is the weak chemical bonding between sodium and oxygen, which is due to the ionic character.

Sodium is bound in more stable sites in glasses containing high-strength cations, like  $\text{Al}_2\text{O}_3$ ,  $\text{B}_2\text{O}_3$ ,  $\text{MgO}$ ,  $\text{ZnO}$  and  $\text{BeO}$ . These oxides have the tendency to act as network formers in tetrahedral configurations. Compensation of the negatively charged  $[\text{AlO}_4]$  or  $[\text{BO}_4]$  tetrahedrons is assured by sodium ions. Tetrahedral configuration of oxides in the glass network is accompanied by a lower free energy, so that sodium ions are trapped in  $\text{Na}[\text{AlO}_4]$  or  $\text{Na}[\text{BO}_4]$  sites.

As a consequence, sodium outlet of glass substrates does not only depend on the concentration gradient, as described above, but also on the type of sodium bondage in the glass structure. Immobilisation of sodium ions by trapping sodium as a charge compensator in tetrahedral-configured oxides is equivalent with a lower chemical potential of sodium as the driving force for diffusion. The concentration gradient can only be seen as the driving force in case of soda–lime–silica glass with sodium bonded at NBO's. In case of boron- or alumina-containing glasses, which are usually used in display technology, close information on glass composition is required to estimate the gradient in chemical potential from the composition. In [10 and 11] elaborated formulas are given to calculate a value that represents the chemical potential and the flux of sodium ions towards the interface glass/coating.

Simplified, the gradient in chemical potential  $\Delta G$  is proportional to the difference of the total amount of sodium ( $\text{Na}_{\text{tot}}$ ) and by sodium trapped at tetrahedral sites ( $\text{Na}[\text{XO}_4]$ ):

$$\Delta G \approx \text{Na}_{\text{tot}} - \text{Na}[\text{XO}_4].$$

In case of  $\text{Na}[\text{XO}_4] \ll \text{Na}_{\text{tot}}$ , e.g. in soda–lime–silica glass, the diffusion is driven by the concentration gradient of sodium. In glasses with sodium excess over boron and aluminium ( $\text{Na}[\text{XO}_4] < \text{Na}_{\text{tot}}$ ) sodium ions diffuse from the glass to the coatings, but the flux of ions is smaller than one would estimate from the concentration gradient. Careful attention has to be paid on glass compositions which result in the formalism  $\text{Na}[\text{XO}_4] > \text{Na}_{\text{tot}}$ . The excess of oxides like  $\text{Al}_2\text{O}_3$  or  $\text{B}_2\text{O}_3$  on  $\text{Na}_2\text{O}$ , which exists in alkali-free or low-alkali glasses, is connected with a high affinity for sodium uptake. SIMS measurements have detected sodium diffusion against the concentration gradient (uphill diffusion), so that silica coatings on Corning Code 7059 glass were purified from sodium impurities [10 and 12]. On the other hand, coatings doped with alkali ions, like in case of the CIS thin film solar cell, have to be protected against loss of sodium by uphill diffusion to the glass substrate.

The two different types of sodium bonding in the glass structure – NBO's and charge compensator in tetrahedral configurations – explain the non-linear sodium outlet from different glass substrates cited in section 1 (figure 1). The stannic oxide thin films with higher sodium concentrations after annealing (samples F and G) are deposited on substrates with a higher sodium content and a lower concentration of  $\text{Al}_2\text{O}_3$  and  $\text{B}_2\text{O}_3$  than in the samples A to E. In glasses F and G, sodium is bonded at NBO's and can easily diffuse. Glass substrates A to E have a lower sodium content, but a higher content of  $\text{Al}_2\text{O}_3$  and  $\text{B}_2\text{O}_3$  in the substrate. Sodium is immobilised at tetrahedral sites of  $\text{R}_2\text{O}_3$ -type substrates.

## 2.3 Interdiffusion mechanism

Up to now the interactions of a glass substrate with thin films during annealing have been discussed considering the diffusive flux of sodium ions only. However, ionic diffusion requires charge balance, i.e. a flux of negatively charged particles in the same direction or of positively charged ions in the opposite direction to sodium ion diffusion.

The only negatively charged species in oxidic glasses is  $\text{O}^{2-}$ , but as oxygen is strongly bonded to the network the diffusion coefficient is too low to assure charge neutrality (table 3). The most probable partner for interdif-

Table 3. Diffusion of ions in oxide glasses (SLS: soda–lime–silica glass) [7]

ion	glasses	$D_0$ in $\text{cm}^2 \text{s}^{-1}$	$Q$ in $\text{kJ mol}^{-1}$	$D_{550^\circ\text{C}}$ in $\text{cm}^2 \text{s}^{-1}$	$x_{550^\circ\text{C}}$ in $\mu\text{m}$
$\text{H}^+$	silica ( $\text{SiO}_2$ )	$1 \cdot 10^{-3}$	66.2	$6 \cdot 10^{-8}$	85
$\text{Na}^+$	silica ( $\text{SiO}_2$ )	0.4	108.0	$5 \cdot 10^{-8}$	80
$\text{Ag}^+$	SLS	$2 \cdot 10^{-2}$	113.1	$1 \cdot 10^{-9}$	12
$\text{O}^{2-}$	silica ( $\text{SiO}_2$ )	$2 \cdot 10^{-9}$	121.4	$4 \cdot 10^{-17}$	0.002

fusion are protons or in general water, as the diffusion coefficients are in the same order of magnitude. The interdiffusion process  $\text{Na}^+$  versus  $\text{H}^+$  was assumed by several workers [3 and 12], but experimental evidence was recently given in connection with investigations on  $\text{TiO}_2$ -coated float glass [13]. A comparison of sodium depth profiling by RBS with hydrogen distribution by NRA revealed that sodium migration is accompanied by a drop of hydrogen in  $\text{TiO}_2$  and proton diffusion into the glass substrate.

As a consequence, contamination of functional coatings by sodium diffusion can be suppressed by limiting hydrogen concentration in thin films. In practice, hydrogen is implemented during deposition, storage or cleaning steps. Furthermore, it is known that oxidic thin films reveal differences in water uptake in dependence on the used material [14]. Concerning proton concentration of thin films, alkali ion migration is a technological as well as a materials problem.

Beside protons, other positive ions present in the coatings can participate in interdiffusion. However, diffusion kinetics is too weak in most cases. Silver, which is used in low-emissivity coating systems for architectural purposes, is an ion that probably concurs with  $\text{H}^+$ .

## 2.4 Sodium diffusion in the coating (diffusion barriers)

In case of a glass composition which tends to sodium outlet due to a gradient in chemical potential, sodium concentration in the coating depends on the deposited material and its properties. In many cases it is necessary to deposit diffusion barriers to protect the functional coatings.

Fundamentals on diffusion barrier coatings can be gained from research activities in the field of semiconductors [15]. In glass technology, different materials [16 to 18] and deposition techniques for diffusion barrier coatings have been reported, but up to now their functioning, above all the influence of deposition technique, impurities and dopants, is not well understood.

The effectivity of a thin film diffusion barrier is strongly connected with its structure, as defects like grain boundaries, cracks or pinholes act as fast diffusion paths. As a consequence, only amorphous materials can be used which have to be deposited with low defect concentration. Furthermore, a diffusion barrier requires

homogeneity in density, composition and thickness over a fixed area. Considering the interdiffusion mechanism, the hydrogen content should be as low as possible. Thus, materials with a low sodium diffusion coefficient in the bulk or amorphous state and a weak affinity to water uptake are required. Concerning technological aspects, high-rate deposition is required to produce homogenous thin films with a controlled defect, impurity and dopant concentration.

Table 4 summarises data for sodium diffusion in different materials which show promise as diffusion barriers. Experimental results on  $\text{Al}_2\text{O}_3$  and  $\text{Si}_3\text{N}_4$  barriers have been published in [12 and 24]. To our knowledge,  $\text{CoO}$  and  $\text{SiAlON}$  compositions have not yet been investigated as diffusion barrier materials on glass.

Considering data of sodium diffusion in silica glass (table 1),  $\text{SiO}_2$  should not be a suitable material for barriers. However, silicon oxide thin films are successfully investigated as diffusion barriers [3 and 12] and commercially available on soda–lime–silica glass [25]. The structural and chemical differences between silica glass and  $\text{SiO}_2$  thin films are not investigated up to now.

Besides deposition of thin films, the chemical modification of glass surfaces is another possibility to create diffusion barriers. Annealing glasses in a reactive gas atmosphere at temperatures above the strain point form a low-sodium, silica-like surface due to dealcalisation [26]. Both the lowered concentration gradient and a silica glass-like structure mean a benefit in minimising alkali ion migration. Another possibility is boron diffusion from precursor substances deposited on the surface [27 and 28]. Tetrahedral-coordinated boron lowers sodium flux towards the interface due to trapping effects at  $[\text{BO}_4]^-$  sites in the glass surface.

## 3. Case study: $\text{CuInSe}_2$ thin film solar cell

The advantage of thin film solar cells over conventionally produced silicon-based products is mainly the aspect of lower costs. Thin film technology means efficient production and lowering the demand of semiconductor materials. Furthermore, expensive high-purity silicon is replaced by copper and indium.

Floated soda–lime–silica glass is used as a cheap substrate material with sufficient mechanical stability, high smoothness and corrosion resistance. Semiconductor developers take advantage of the existing practical and technological experience in handling, cleaning, coating and tempering of flat glass gained in industrial large-area refining of flat glass.

In the following, the setup and processing of a thin film solar cell on the basis of  $\text{CuInSe}_2$ , commonly abbreviated as CIS, is shortly described [29].

### 3.1 Processing

After cutting and cleaning of floated soda–lime–silica glass, the substrates are transferred into a vacuum coat-

Table 4. Sodium diffusion in different materials

material	$D_0$ in $\text{cm}^2 \text{s}^{-1}$	$Q$ in $\text{kJ mol}^{-1}$	$D_{550^\circ\text{C}}$ in $\text{cm}^2 \text{s}^{-1}$	$x_{550^\circ\text{C}}$ in nm	reference
CoO (single crystal)	$8.1 \cdot 10^{-2}$	206.0	$6.9 \cdot 10^{-15}$	29	[19]
Mo (single crystal)	$3.0 \cdot 10^{-9}$	89.0	$6.7 \cdot 10^{-15}$	28	[20]
a-SiON:H (17% O)	$4.3 \cdot 10^{-5}$	155.9	$5.5 \cdot 10^{-15}$	26	[21]
$\text{Al}_2\text{O}_3$ (single crystal)	$2.0 \cdot 10^{-2}$	209.4	$1.1 \cdot 10^{-15}$	11	[22]
SiAlON glass	$2.4 \cdot 10^{-4}$	178.7	$1.1 \cdot 10^{-15}$	11	[23]
a-SiON:H (0% O)	$1.4 \cdot 10^{-4}$	176.2	$8.9 \cdot 10^{-16}$	10	[21]

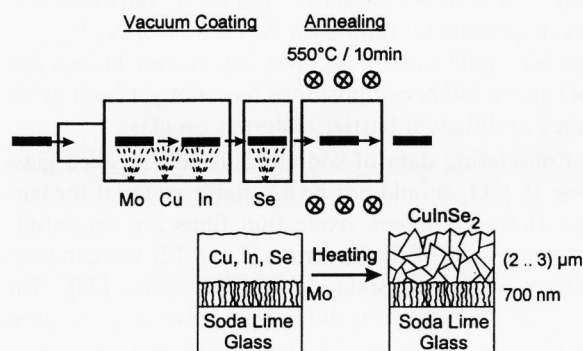


Figure 3. Processing of a CIS thin film solar cell (RTP) [29].

ing chamber (figure 3). Molybdenum, copper and indium are deposited sequentially by dc-magnetron sputtering. Selenium is added in a second step by thermal evaporation. The float glass coated with the precursor is heat-treated to form  $\text{CuInSe}_2$ , which is the photovoltaic active composition. Phase development requires rapid thermal processing (RTP) in 10 min annealing at  $550^\circ\text{C}$  with high heating and cooling rates. Parameters in RTP are very similar to the tempering of float glass, so that the technological experience from producing safety glass can be used. In the next step, a thin buffer layer of CdS and ZnO as a transparent conductive oxide is deposited. The multilayer system is protected against environmental influences by fixing a second low-absorption glass pane with a polymeric foil.

A critical step in processing is the tempering of the coated glass. The temperature is with  $550^\circ\text{C}$  slightly higher than the transformation point of floated soda–lime–silica glass. The mobility of sodium ions is high enough to diffuse through the molybdenum back contact into the CIS absorber. Sodium influences the grain growth [30] as well as the electrical conductivity of  $\text{CuInSe}_2$  [31]. Sodium impurity diffusion from the glass substrate during RTP results in a rise in conversion efficiency of the CIS solar cell [32]. Optimising sodium concentration or at least adjusting a constant sodium level in the absorber layer is hard to control by outdiffusion from the glass substrate. As a consequence sodium has to be doped during deposition to get optimised device characteristics. Hence, it is necessary to minimise alkali ion migration from the glass substrate during RTP. As it is discussed above, there are in principle several ways to minimise sodium contamination of the  $\text{CuInSe}_2$  layer:

- deposition on alkali-free substrates or
- low-sodium glasses, which immobilise sodium,
- diffusion barrier coatings between the substrate and the molybdenum back contact and
- chemical modification of glass surfaces, e.g. dealcalization and boron treatment.

In case of the CIS thin film solar cell, sodium outlet of different commercially available substrates is compared and discussed considering the relation between glass chemistry and sodium diffusion. CVD- and sputter-deposited diffusion barriers on soda–lime–silica glass are investigated and compared with dealcalized glass surfaces.

### 3.2 Glass substrates with a minimised outlet of alkali ions

Which types of commercially available glasses can be used as substrate materials that guarantee no or at least weak interactions between glass surface and functional coatings? Concerning this question, intensive research has been done in the last decade in the field of display technology [33 to 37].

Table 5 summarises the maximum process temperature as well as physical properties of commercially available flat glasses. We distinguish between alkali-containing glasses, like soda–lime–silica glass, borosilicate glass (Borofloat<sup>TM</sup>) or alkaline aluminosilicate glass (Corning Code 0371<sup>TM</sup>) and alkali-free glasses. The latter are divided into boroaluminosilicate glasses (Corning Code 7059<sup>TM</sup>), alkaline earth aluminosilicate glasses and silica glass at process temperatures higher than  $800^\circ\text{C}$ .

Processing at temperatures higher than  $600^\circ\text{C}$  requires one of the expensive alkali-free glasses, but below soda–lime–silica glass in combination with an effective surface passivation shows promise as a cheap substrate material.

The choice of a suitable substrate for the CIS thin film solar cell depends on

- first, physical properties, i.e. a coefficient of thermal expansion in the range of  $\alpha \approx (8 \text{ to } 9) \cdot 10^{-6} \text{ K}^{-1}$  and a strain point higher than  $520^\circ\text{C}$ ,
- second, the price and availability of the glass,
- third, the costs for refining with diffusion barriers in case of sodium-containing glasses.

Table 5. Maximum process temperature ( $\vartheta_{\max}$ ) and physical properties of different flat glass compositions

glass	$T_g$ in °C	$\vartheta_{\max}$ in °C	$\alpha$ in $10^{-6} \text{ K}^{-1}$	glass composition
silica	1200	1250	0.5	$\text{SiO}_2$
Corning 1729	800	850	3.5	alkaline earth aluminosilicate
Corning 1724	660	710	4.3	boroaluminosilicate
Corning 1733	640	690	3.7	boroaluminosilicate
Corning 7059	593	643	4.6	boroaluminosilicate
Corning 0371	574	624	8.8	alkali-containing
soda–lime–silica	540	590	9.0	alkali-containing
Borofloat (Schott)	530	580	3.3	alkali-containing
Corning 0211 (microsheet)	508	558	7.4	alkali-containing

Table 6. Composition of substrate glasses in wt% (SLS: soda–lime–silica glass)

glass	$\text{SiO}_2$	$\text{B}_2\text{O}_3$	$\text{Al}_2\text{O}_3$	$\text{Na}_2\text{O}$	$\text{K}_2\text{O}$	$\text{CaO}$	$\text{MgO}$	$\Sigma\text{R}_2\text{O}_3$
SLS <sup>3)</sup>	72.2		0.6	13.0	0.4	8.7	4.2	0.6
Borofloat <sup>TM 3)</sup>	83.7	10.0	2.4	3.5	0.7			12.4
0371 <sup>3)</sup>	60.4		17.1	12.3	3.5	0.3	3.2	17.1
7059	49	15	10					25
1733	57	12	15					27
1724	57	5	16					21
1729	66		19					19

<sup>3)</sup> Determined by X-ray fluorescence analysis.

Soda–lime–silica glass and Corning Code 0371<sup>TM</sup> glass match the demands in thermal expansion and availability. Both glasses, which are nearly identically in sodium content, are tested as substrates in the present work. Borofloat<sup>TM</sup> is investigated as a substrate with a lower sodium content, although the coefficient of thermal expansion does not match the requirements. The compositions of several commercially available flat glasses, including the investigated substrates, are given in table 6.

### 3.3 Sodium diffusion in molybdenum thin films

What is the reason for the high permeability of the molybdenum back contact to sodium diffusing from the glass substrate? The diffusion coefficient of sodium in molybdenum is comparatively low (table 4) and the molybdenum back contact has a higher thickness than the tested diffusion barrier coatings (table 7), so in principle the molybdenum layer could have barrier properties.

Thin films of metals with a high melting point grow with columnar structure. Within the refractory metals like tungsten, rhenium, osmium, tantalum or molybdenum the diameter of the columns decreases with increasing melting point [15]. Thus the sputtered molyb-

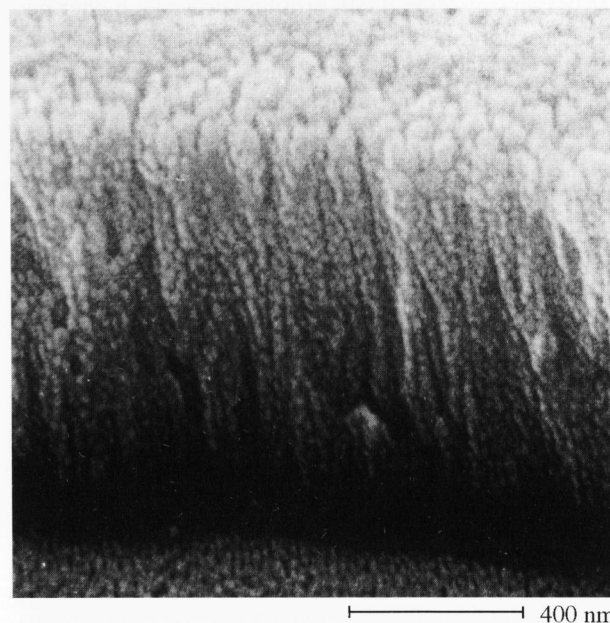


Figure 4. SEM micrograph of the column structure of the molybdenum back contact.

denum back electrode grows with a pronounced orientation vertical to the glass surface as it can be seen in SEM (figure 4). Sodium diffusion from the substrate into the CIS absorber during RTP occurs via grain boundaries which act as fast diffusion paths.

Sodium diffusion in the molybdenum thin film can be suppressed to a certain extent by stress optimisation. Samples prepared with compressive stress reveal lower sodium concentration in XPS measurements compared to molybdenum coatings under tensile stress [32].

Table 7. Thickness (in nm) of the investigated coatings

$\text{AlN}_x$	$\text{Al}_2\text{O}_3$	$\text{BiO}_x$	$\text{SiO}_x$	$\text{SiN}_x\text{:H}$	Mo
30	30	30	200	250	700

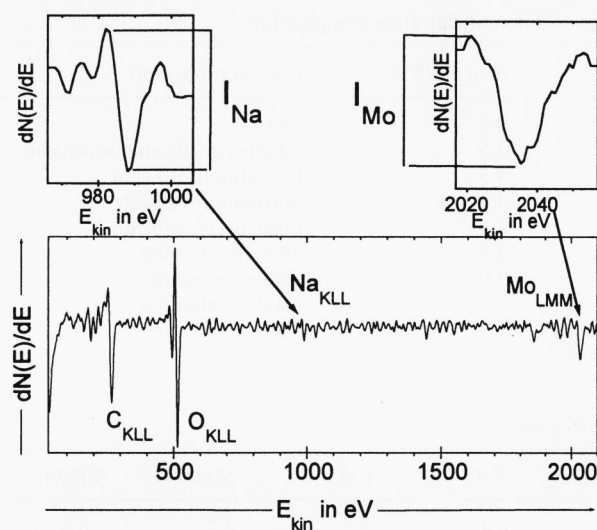


Figure 5. Semi-quantitative determination of sodium surface concentration of annealed samples (AES). The shift of the  $Mo_{LMM}$  peak from 2044 to below 2040 eV is related to the formation of molybdenum oxide at the surface.

In a recent publication [38], the influence of the oxygen in sputtered molybdenum films on sodium diffusion from soda–lime–silica glass substrates was examined. SIMS concentration depth profiling proved a higher permeability in molybdenum coatings with rising oxygen content. Molybdenum oxide phases at the grain boundaries are proposed as intercalation hosts for sodium, as  $MoO_3$  is an electrochromic oxide. Considering charge neutrality which requires a counterflow of protons, the absorption of humidity in the molybdenum oxides at the grain boundaries is probably the determining factor. A higher oxygen concentration is equivalent with rising hydrogen concentration, bound either at intercalation sites ( $H_x/Na_x$ ) $MoO_3$  or hydroxylic groups  $MoO_3(OH/Na)$ .

### 3.4 Experimental

Sodium ion migration from different compositions (table 6) or passivated soda–lime–silica glass was determined by AES. Coated glass samples were tempered 10 min at different temperatures up to 650 °C in helium atmosphere in case of molybdenum (RTP) and in air in case of oxidic or nitridic diffusion barrier materials (laboratory kiln). Sodium concentration on sample surfaces after annealing was determined semi-quantitatively by relating the sodium Auger signal ( $E_{kin} = 990$  eV) to the constant intensity of a reference element, e.g. molybdenum ( $E_{kin} = 2044$  eV), as it is illustrated in figure 5. The investigated diffusion barrier materials which differ in chemical composition were half-coated with a thin gold layer after annealing. The samples were positioned in the AES in a way that allows to get 50 % information from the original sample surface, containing the elements of the diffusion barrier as well as sodium, and the other part from the gold-coated side as a reference ( $E_{kin} = 2024$  eV).

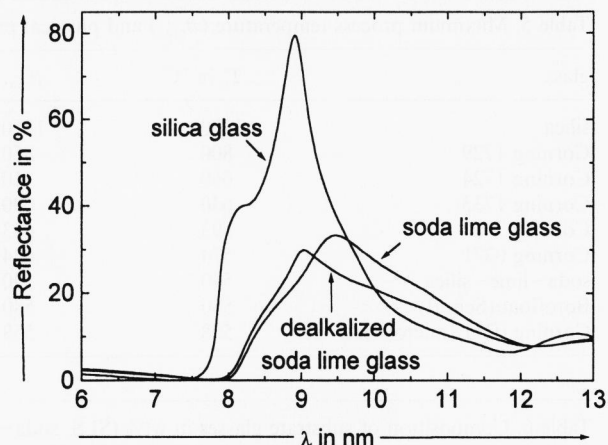


Figure 6. Formation of bridging oxygens during dealcalisation in HCl/Ar at 700 °C for 30 min (FTIR).

Insulating samples, i.e. all investigated oxidic and nitridic coated glasses were tilted to an angle of incidence of 30° between sample surface and electron beam to avoid spectra shift due to sample charging. Charge effects were also minimised by applying a low acceleration voltage ( $E_p = 5$  kV) and a low beam current ( $I_p = 10$  nA). Conductively molybdenum-coated glasses were measured under 90° incidence with  $E_p = 10$  kV and  $I_p = 10$  nA. Structural characterisation of the coatings was performed by GI-XRD with the diffractometer D 500 of Siemens AG, München (Germany).

Topography is important to describe changes in thin films during annealing, above all crack propagation. High-resolution SEM investigations were carried out with a Cambridge Instruments Stereoscan MK3, Cambridge (UK). The investigated films were prepared by dc-magnetron ( $AlN_x$ , Mo), rf-sputter deposition ( $Al_2O_3$ ) and CVD ( $SiN_x:H$ ,  $SiO_x$ ). Film thickness is summarized in table 7.

Dealcalization of soda–lime–silica glass was carried out by annealing samples in a continuous HCl/Ar gas flow in a silica glass tube. FTIR measurements to detect bridging oxygens in  $SiO_2$  formation in the surface showed best results after 30 min annealing at 700 °C (figure 6).

### 3.5 Sodium outlet from different substrates

The glass slides were coated with 700 nm molybdenum and annealed for 10 min in helium atmosphere at different temperatures under conditions of RTP.

In case of soda–lime–silica glass substrates, sodium diffusion through the molybdenum coating is detectable by AES at temperatures above 250 °C (figure 7). In the range of the strain point, i.e. above 530 °C, sodium outlet is forced due to rising mobility of the ions in the glass. Alkali aluminosilicate glass has a lower tendency of sodium outlet, although the sodium content of both glasses is nearly the same. Sodium segregation is not de-



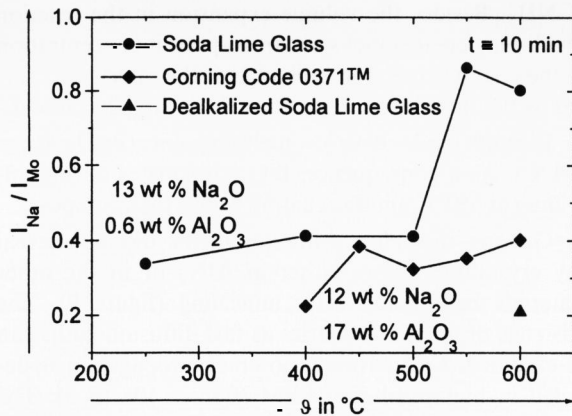


Figure 7. Sodium outlet from soda–lime–silica glass, dealkalised soda–lime–silica glass, alkali aluminosilicate (Corning Code 0371™) and borosilicate glass (Borofloat™) determined by AES. The substrates are coated with 700 nm molybdenum. The Borofloat sample is below detection limit.

tectable until 400°C. The strain point of the alkali aluminosilicate glass is 580°C, so the sodium concentration at the molybdenum surface does not show the increase like the soda–lime–silica glass. No sodium was detected up to 600°C in case of borofloat™. The surface sodium concentration may be beyond the detection limit of AES (3 to 5 at.%) as the sodium content of this substrate is with 3.5% comparatively low.

Soda–lime–silica and alkali aluminosilicate glass are examples for the influence of sodium bonding on the  $H^+/Na^+$  ion exchange. Sodium in soda–lime–silica glass is well known to be bound at NBO's, which are the pinpoints for ionic diffusion. In case of alkali aluminosilicate glass, sodium ions are used as charge compensators for the formation of negatively charged  $[AlO_4]$  tetrahedrons, which act as network formers. Only excess sodium bound at NBO's is able to diffuse.

The gradient in chemical potential of sodium can be estimated from the difference of the sodium content of the glass ( $Na_{tot}$ ) and sodium immobilised at tetrahedral sites ( $Na[XO_4]$ ). Soda–lime–silica glass contains 25.2 mol% sodium ions and 0.7 mol% aluminium ions, so the difference is

- $Na_{tot} \approx Na[XO_4] \approx +24.5$  in the case of soda–lime–silica glass, and analogously
- $Na_{tot} \approx Na[XO_4] \approx +4.0$  (alkali aluminosilicate Corning Code 0371™),
- $Na_{tot} \approx Na[XO_4] \approx -13.5$  (borofloat™).

The high positive value of soda–lime–silica glass indicates that the gradient in chemical potential is nearly identical with the gradient of sodium concentration. As a consequence, a strong diffusive flux of sodium ions into the coating is observed (figure 7). In case of alkali aluminosilicate glass, the difference results in a low positive value. Sodium diffusion into the coating occurs, but the particle flux is much less comparing with soda–lime–silica glass. Borofloat™ has a negative value, which means that there is no sodium outlet from the

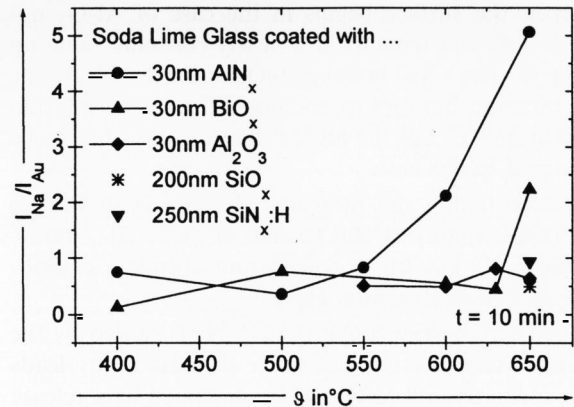


Figure 8. Temperature dependence of diffusion barrier properties of different oxidic and nitridic coatings (AES).

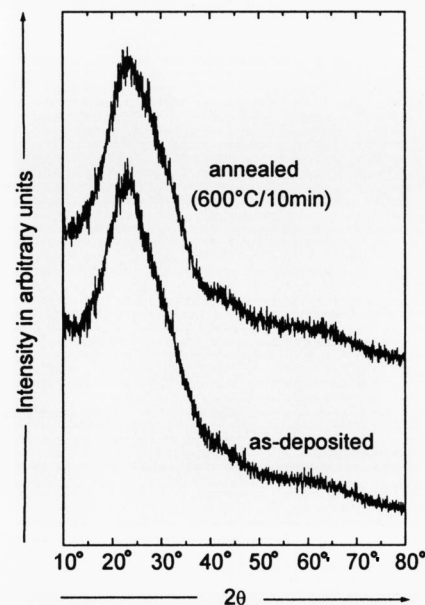


Figure 9. Diffraction diagrams of 30 nm  $AlN_x$ , deposited on soda–lime–silica glass (GI-XRD).

substrate. Three coordinated boron or alumina is left in the glass due to the low sodium content. This substrate probably tends to uphill diffusion of sodium.

### 3.6 Testing of diffusion barrier coatings

$AlN_x$ ,  $BiO_x$ ,  $Al_2O_3$ ,  $SiO_x$ ,  $SiN_x:H$  thin films are examined as diffusion barrier coatings on soda–lime–silica glass. The samples are annealed 10 min at different temperatures in a laboratory kiln at ambient atmosphere.

Differences in permeability for sodium from the glass substrate are illustrated in figure 8.  $AlN_x$  shows rather poor barrier properties. An exponential increase of sodium concentration at the sample surface with rising temperature is observed.  $BiO_x$  reveals agreeable barrier properties up to 630°C. Higher temperatures are not recommended as the Na: Au ratio increases. Sodium segre-

gation at the surface begins in the case of  $\text{Al}_2\text{O}_3$  not until  $550^\circ\text{C}$  and remains at a nearly constant value up to  $650^\circ\text{C}$ . The CVD coatings  $\text{SiO}_x$  and  $\text{SiN}_x\text{:H}$  are the best diffusion barriers as sodium diffusion is only detected at  $650^\circ\text{C}$ , but the higher film thickness has to be considered in this case.

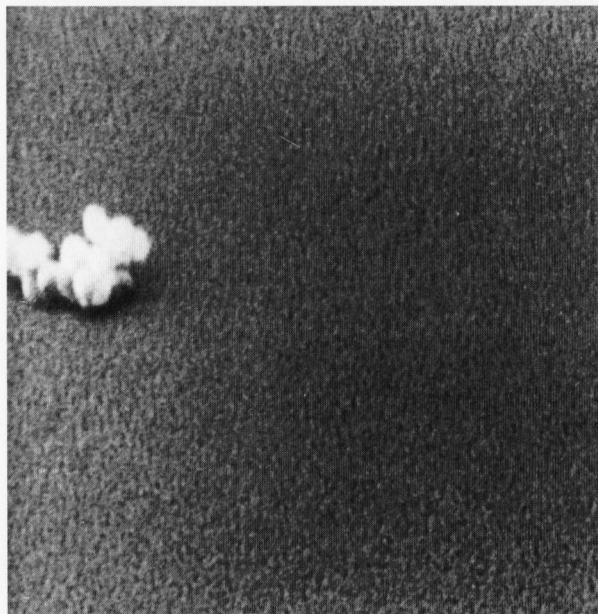
Substantiating the measured differences in barrier properties requires careful research on materials characterisation of thin films, considering chemical composition as well as structural aspects.

The weak barrier property of  $\text{AlN}_x$  is caused by the high reactivity of  $\text{AlN}$  with water [39]. Humidity leads to the formation of  $\text{Al}(\text{OH})_3$ , accompanied by a release

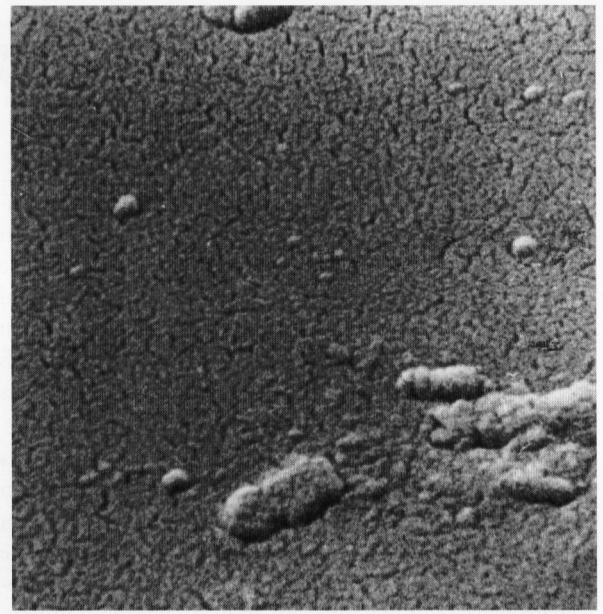
of  $\text{NH}_3$ . Besides the volume expansion in the reaction which may create cracks or stress, proton concentration of the coating rises. Ion exchange at the interface is forced as the interdiffusion partner  $\text{H}^+$  is already present.

Bismuth oxides have low melting points ( $\text{Bi}_2\text{O}_3$ :  $\vartheta_m = 704^\circ\text{C}$ ). As a consequence,  $\text{BiO}_x$  sublimates during annealing at  $650^\circ\text{C}$  and the coating begins to decompose.

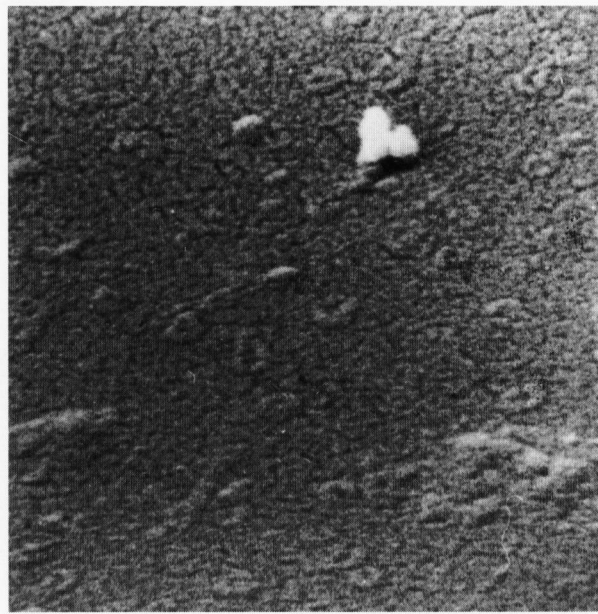
Grazing incidence diffractometry did not reveal any crystalline phases either in  $\text{AlN}_x$  or in the other materials before and after annealing (figure 9). The existence of grain boundaries as fast diffusion paths can be excluded. Furthermore, no crack propagation is detected in high-resolution SEM (figures 10a to d). The



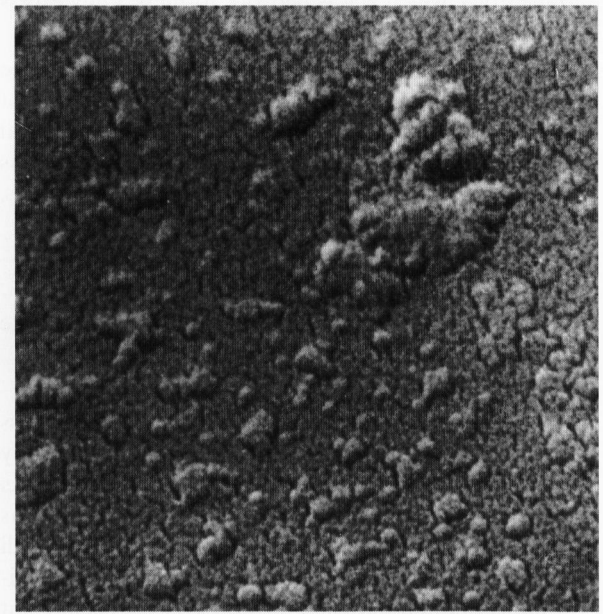
a) 400 nm



b) 400 nm



c) 400 nm



d) 400 nm

Figures 10a to d. High resolution SEM images of as-deposited and annealed  $\text{Al}_2\text{O}_3$  coatings (figures a and b) and of as-deposited and annealed  $\text{AlN}_x$  coatings (figures c and d), respectively. Annealing conditions:  $600^\circ\text{C}/10$  min in air.

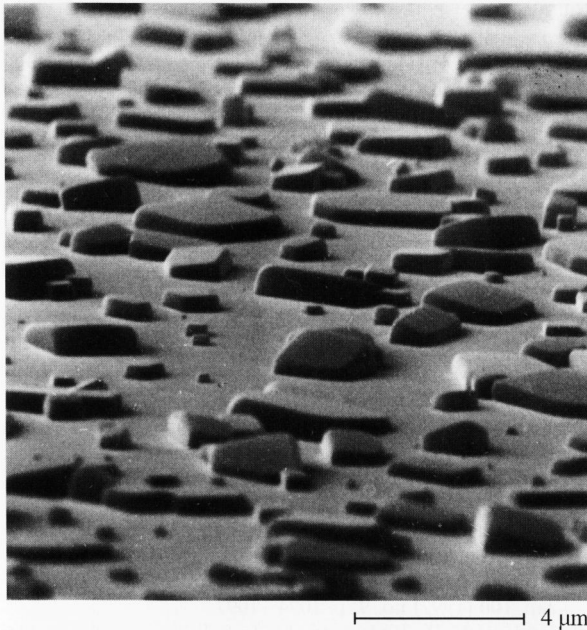


Figure 11. SEM image of a dealkalised soda–lime–silica glass surface.

differences in barrier properties between  $\text{Al}_2\text{O}_3$  and  $\text{BiO}_x$  (up to  $630^\circ\text{C}$ ) and both CVD coatings are assumed to be mainly due to the effect of film thickness.

Deposition technique and parameters strongly influence defect concentration, microstructure, density or impurities in thin films. As there are only a few publications concerning these questions in the field of diffusion barrier coatings [3 and 16], intensive research is required to optimise and understand the mechanisms of barriers.

Float glass surfaces have been successfully dealkalised at  $700^\circ\text{C}$  in an HCl atmosphere. Flat NaCl crystallites of the size of several micrometres could be detected by SEM on top of the treated glass surfaces (figure 11). After removing the hazy salt layer by washing with deionised water, the samples were coated with metallic molybdenum (thickness 700 nm). Afterwards, the samples were annealed for 10 min under RTP conditions at 400, 500, 550 and  $600^\circ\text{C}$ , respectively. Figure 7 reveals that sodium is detectable only at the surface of the sample annealed at  $600^\circ\text{C}$ . The sodium concentration on top of the molybdenum film is strongly reduced compared to the molybdenum-coated soda–lime–silica glass or the Corning glass. This shows that the dealkalised float glass surfaces act as excellent barriers against sodium diffusion.

#### 4. Conclusion

In principle, there are several ways to minimise alkali ion migration from flat glass substrates into functional coatings on glass:

- a) Utilizing glass substrates with low sodium diffusion coefficient.

Considering the correlations between glass composition and sodium diffusion, these glasses should be low-sodium alkaline-earth boroaluminosilicate glasses. Diffusion data reveal that the effect of lowering sodium mobility by compositional variations is too weak. Lowering the concentration gradient is one possibility to minimise sodium migration, the other is trapping sodium as a charge compensator in tetrahedral sites of boron or aluminium. In any case, the driving force in ionic diffusion is the chemical potential.

- b) Removal of protons as the diffusion partner.

Sodium outlet of glass substrates is accompanied by a counter flow of protons to assure charge neutrality. Water content in the coatings, incorporated during deposition, storage, or annealing in a humid atmosphere forces sodium diffusion. In this connection, there is some uncertainty about hydrogen in  $\text{SiO}_2$  diffusion barrier coatings, as there are hints given in literature that hydrogen improves barrier properties.

- c) Surface passivation with diffusion barriers.

Soda–lime–silica glass, which shows promise as a cheap substrate material, requires effective surface passivation. Barriers which protect functional coatings against sodium incorporation have to be deposited amorphous with low defect concentration. According to diffusion data alumina, silicon nitride,  $\text{SiAlON}$  compositions and cobalt oxide can be used presupposed that they are deposable economically and defect-free.  $\text{SiO}_2$  thin films are commonly used, although they should not be able to block sodium according to diffusion data of sodium in silica glass. The structural or chemical differences between silica glass and  $\text{SiO}_2$  thin films are not clear up to now. Another effective possibility in passivating soda–lime–silica glass is dealkalising the surface by annealing in a reactive atmosphere. Sodium is extracted by HCl or  $\text{SO}_2$  and a silica-rich surface layer with excellent barrier properties is formed.

Different ways in alkali ion migration control are investigated in the case of the CIS thin film solar cell.

Sodium outlet from molybdenum-coated soda–lime–silica glass, Corning Code 0371<sup>TM</sup> alkali aluminosilicate glass and floated borosilicate glass (Borofloat<sup>TM</sup>) is determined by AES. Borofloat<sup>TM</sup> did not reveal any sodium concentration at the surface of annealed samples, but the coefficient of thermal expansion is too low to be used in the present application. The alkali aluminosilicate glass immobilises sodium to a certain extent at tetrahedral sites of aluminium. As a consequence, sodium outlet is much less from Corning Code 0371<sup>TM</sup> compared to floated soda–lime–silica glass, although the sodium content of both glasses is nearly identical. In case of both glass substrates a surface passivation is necessary to protect the CIS thin film from sodium in-

corporation. As a consequence, the less expensive soda–lime–silica glass will be the choice for the solar cell from the economic point of view.

Several sputter-deposited thin films of the thickness 30 nm and CVD coatings (200 to 250 nm) were tested as diffusion barriers on soda–lime–silica glass. The CVD coatings  $\text{SiO}_x$  and  $\text{SiN}_x\text{:H}$  as well as sputter-deposited  $\text{Al}_2\text{O}_3$  and  $\text{BiO}_x$  (up to 630 °C) showed agreeable barrier properties.  $\text{AlN}_x$  is highly permeable to sodium from the substrate as it reacts with humidity. Sodium diffusion in  $\text{AlN}_x$  is forced by rising proton concentration.

Dealkalisation of soda–lime–silica glass by annealing in HCl atmosphere leads to silica-rich surfaces with excellent barrier properties. In production of flat glass, soda–lime–silica glass is always dealkalised to a certain extent by evaporation of sodium and extraction by  $\text{SO}_2$  from the exhaust gas. This effect could be intensified in float lines by blowing the surfaces with reactive gas in the cooling region.

\*

We would like to express our thanks to the CIS team at Siemens Solar, München (Germany). F. Karg and W. Riedl took care of a fruitful cooperation within the FORSOL research programme. W. Stetter supplied us reliably with different sets of samples. R. Rox and M. Schmidt from Interpane Glas Industrie AG, Lauenförde (Germany), enabled us to deposit barrier materials in large-area coaters. The help of Dr. H. Göbel, Laboratory of Crystallographic Analytics, München, who carefully carried out the X-ray investigations of our films, is greatly appreciated. We also thank H. Hildebrand for her patient assistance at numerous Auger measurements, and E. Springer for SEM imaging.

The financial support by the Bayerische Forschungsstiftung and by the Bayerisches Staatsministerium für Landesentwicklung und Umweltfragen is gratefully acknowledged.

## 5. References

- [1] Bach, H.; Schroeder, H.: Kristallstruktur und optische Eigenschaften von dünnen, organogenen Titanoxyd-Schichten auf Glasunterlagen. *Thin Solid Films* **1** (1967/68) no. 4, p. 255–276.
- [2] Mizuhashi, M.: Electrical properties of  $\text{SnO}_2$  films on various substrates. *J. Non-Cryst. Solids* **38 & 39** (1980) p. 329–334.
- [3] Mizuhashi, M.; Gotoh, Y.; Matsumoto, K. et al.: Migration of alkali ions from glass substrates with and without barrier coating. *Rep. Res. Lab. Asahi Glass Co., Ltd.* **36** (1986) no. 1, p. 1–14.
- [4] Mattox, D. M.: Sol-gel derived, air baked indium and tin oxide films. *Thin Solid Films* **204** (1991) p. 25–32.
- [5] Terai, R.; Hayami, R.: Ionic diffusion in glasses. *J. Non-Cryst. Solids* **18** (1975) p. 217–264.
- [6] Doremus, R. H.: *Glass science*. New York (et al.): Wiley, 1973.
- [7] Frischat, G. H.: *Ionic diffusion in oxide glasses*. Bay Village, OH (USA); Aedermannsdorf (Switzerland): *Trans Tech Publ.*, 1975.
- [8] Frischat, G. H.: Ionentransport in Siliciumdioxid. *Glastech. Ber.* **45** (1972) no. 7, p. 309–319.
- [9] Schaeffer, H. A.; Mecha, J.; Steinmann, J.: Mobility of sodium ions in silica glass of different OH content. *J. Am. Ceram. Soc.* **62** (1979), no. 78, p. 343–346.
- [10] Araujo, R. J.; Fehlner, F. P.: Sodium redistribution between oxide phases. *J. Non-Cryst. Solids* **197** (1996) p. 154–163.
- [11] Fehlner, F. P.: Thin Films on Glass for Liquid Crystal Displays. *J. Non Cryst. Solids* **218** (1997), p. 360–367.
- [12] Fehlner, F. P.; Salisbury, K. R.; Binkowski, N. J.: Barrier layers for LCD glass. *SID (Society for Information and Display) Dig., Tech. Papers* **26** (1995) p. 771–774.
- [13] Laube, M.: Einfluß der Umgebungsbedingungen auf die Elementverteilung in Floatglasoberflächen und Beschichtungen. *Johann Wolfgang Goethe-Universität Fachber. Physik, Frankfurt/M., Diss.* 1996.
- [14] Wagner, W.; Rauch, F.; Bange, K.: Concentration profiles of hydrogen in technical oxidic thin films and multilayer-systems. *Fresenius Z. Anal. Chem.* **333** (1989) p. 478–480.
- [15] Nicolet, M.-A.: Diffusion barriers in thin films. *Thin Solid Films* **52** (1978) p. 415–443.
- [16] Mizuhashi, M.; Gotoh, Y.: Effect of silicon oxide coatings on the out-diffusion of alkali from soda–lime–silica glass. *Rep. Res. Lab. Asahi Glass Co., Ltd.* **32** (1982) no. 2, p. 79–86.
- [17] Matsuda, A.; Matsuno, Y.; Katayama, S. et al.: Alkali passivation mechanism of sol-gel derived  $\text{TiO}_2$ - $\text{SiO}_2$  films coated on soda–lime–silica glass substrates. *J. Ceram. Soc. Jap.* **100** (1992) no. 9, p. 1094–1097.
- [18] Fehlner, F. P.; Binkowski, N. J.; Salisbury, K. R. et al.: Alumina barrier layers on LCD glass. *J. Non-Cryst. Solids* **195** (1996) p. 89–94.
- [19] Hoshino, K.; Peterson, N. L.: Cation impurity diffusion in CoO and NiO. *J. Phys. Chem. Solids* **45** (1984) no. 8–9, p. 963–974.
- [20] Dubinin, G. N.; Benediktova, G. P.; Karpman, M. G. et al.: Diffusion of alkali metals in refractory metals. (*Orig. Russ.*) *Khim.-Term. Obrab. Stali Splavov* **6** (1969) p. 129–137.
- [21] Osenbach, J. W.; Voris, S. S.: Sodium diffusion in plasma-deposited amorphous oxygen-doped silicon nitride ( $\text{a-SiON:H}$ ) films. *J. Appl. Phys.* **63** (1988) p. 4494–4500.
- [22] Frischat, G. H.: Kationentransport in Aluminiumoxid. *Ber. Dt. Keram. Ges.* **48** (1971) no. 10, p. 441–447.
- [23] Das, T.; Sanyal, A. S.; Mukerji, J.: Diffusion of  $^{22}\text{Na}$  and  $^{59}\text{Fe}$  in Mg-Si-Al-O-N glasses. *Phys. Chem. Glasses* **35** (1994) no. 5, p. 198–201.
- [24] Dürdoth, P.; Slowik, J.; Borchardt, G. et al.: Lebensdauer von Beschichtungen auf Massengläsern. *Abschlußbericht zum AiF-Forschungsvorhaben Nr. 7859. TU Clausthal Fachber. Metallurgie und Werkstoffwissenschaften*, 1992.
- [25] Faulkner, E. K.; Whitney, R. K.; Zeman, J. E.: Alkali extraction as a determinant in the selection of a glass for displays. *IEEE Trans. Electron Devices* **ED-30** (1983) no. 5, p. 545–548.
- [26] Schaeffer, H. A.; Stengel, M.; Mecha, L.: Dealkalization of glass surfaces utilizing HCl gas. *J. Non-Cryst. Solids* **80** (1986) p. 400–404.
- [27] Yoldas, B. E.; Hanson, M. E.; Duffer, P. F.: Formation of an alkali diffusion barrier glass surface. In: *Proc. XVII International Congress on glass, Beijing (P. R. China) 1995. Vol. 4.* p. 73–78.
- [28] Yoldas, B. E.: Optical and chemical modification of float glass surfaces. In: *Proc. International Symposium on Glass Problems.* (1996) Vol. 1. p. 455–461.
- [29] Karg, F.; Probst, V.; Harms, H. et al.: Novel rapid-thermal-processing for CIS thin-film solar cells. In: *Proc. 23rd IEEE Photovoltaic Specialists Conference 1993.* p. 441–446.
- [30] Bodegård, M.; Stolt, L.; Hedström, J.: The influence of sodium on the grain structure of  $\text{CuInSe}_2$  films for photovoltaic applications. In: *Proc. 12th European Photovoltaic Solar Energy Conference 1994.* p. 1743–1746.
- [31] Holz, J.; Karg, F.; Phillipsborn, H. v.: The effect of substrate impurities on the electronic conductivity in CIS thin films. In: *Proc. 12th European Photovoltaic Solar Energy Conference, 1994.* p. 1592–1595.

- [32] Probst, V.; Rimmasch, J.; Riedl, W. et al.: The impact of controlled sodium incorporation on rapid thermal processed Cu(InGa)Se<sub>2</sub>-thin films and devices. In: Proc. 1st World Conference on Photovoltaic Energy Conversion, Hawaii 1994, p. 144–147.
- [33] Dumbaugh, W. H.; Bocko, P. L.; Fehlner, F. P.: Glasses for flat-panel displays. In: Cable, M.; Parker, J. M. (eds.): High-performance glasses. Glasgow, London: Blackie, 1992, p. 86–101.
- [34] Fehlner, F. P.; Dumbaugh, W. H.; Miller, R. A.: Refractory Glass substrates for thin film transistors. *Jap. Display* (1986) p. 200–203.
- [35] Dumbaugh, W. H.; Bocko, P. L.: Substrate glasses for flat-panel displays. *SID (Society for Information and Display) Dig., Tech. Papers* (1990) p. 70–72.
- [36] Lapp, J. C.; Bocko, P. L.; Nelson, J. W.: Advanced glass substrates for flat panel displays. *SPIE* **2174** (1994) p. 129–138.
- [37] Moffat, D. E.: Properties of glass substrates for poly-Si AMLCD technology. In: Proc. Materials Research Society Symposium, 1995. Vol. 377. p. 871–876.
- [38] Grannath, K.; Stolt, L.; Bodegård, M. et al.: Sodium in sputtered Mo back contacts for Cu(In, Ga)Se<sub>2</sub> devices: Incorporation, diffusion, and relationship to oxygen. In: Proc. 14th European Photovoltaic Solar Energy Conference, 1997.
- [39] Hotza, D.; Sahling, O.; Greil, P.: Hydrophobing of aluminium nitride powders. *J. Mater. Sci.* **30** (1995) p. 127–132.

■ 0500P003

## Addresses of the authors:

N. Janke  
Vegla GmbH, Produktentwicklung  
Viktoriaallee 3–5  
D-52066 Aachen

O. Grassmé, R. Weissmann  
Institut für Werkstoffwissenschaften III  
Lehrstuhl Glas und Keramik  
Universität Erlangen-Nürnberg  
Martensstraße 5  
D-91066 Erlangen